Journal of Biomechanics 150 (2023) 111479

Contents lists available at ScienceDirect

Journal of Biomechanics

journal homepage: www.elsevier.com/locate/jbiomech

Strain-dependent elastography of cancer cells reveals heterogeneity and stiffening due to attachment

Wenwei Xu [a,1], Saif Kabariti [a,1], Katherine M. Young [b], Steven P. Swingle [a], Alan Y. Liu [a], Todd Sulchek [a,b,*]

[a] George W. Woodruff School of Mechanical Engineering, Georgia Institute of Technology, Atlanta, GA 30332 USA
[b] Wallace H. Coulter Department of Biomedical Engineering, Georgia Institute of Technology, Atlanta, GA 30332 USA

ARTICLE INFO

Keywords:
Atomic force microscopy
Cancer cell mechanics
Cellular biophysics
Elastic moduli
Actin cytoskeleton

ABSTRACT

Because cells vary in thickness and in biomechanical properties, the use of a constant force trigger during atomic force microscopy (AFM) stiffness mapping produces a varied nominal strain that can obfuscate the comparison of local material properties. In this study, we measured the biomechanical spatial heterogeneity of ovarian and breast cancer cells by using an indentation-dependent pointwise Hertzian method. Force curves and surface topography were used together to determine cell stiffness as a function of nominal strain. By recording stiffness at a particular strain, it may be possible to improve comparison of the material properties of cells and produce higher contrast representations of cell mechanical properties. Defining a linear region of elasticity that corresponds to a modest nominal strain, we were able to clearly distinguish the mechanics of the perinuclear region of cells. We observed that, relative to the lamelopodial stiffness, the perinuclear region was softer for metastatic cancer cells than their nonmetastatic counterparts. Moreover, contrast in the strain-dependent elastography in comparison to conventional force mapping with Hertzian model analysis revealed a significant stiffening phenomenon in the thin lamellipodial region in which the modulus scales inversely and exponentially with cell thickness. The observed exponential stiffening is not affected by relaxation of cytoskeletal tension, but finite element modeling indicates it is affected by substrate adhesion. The novel cell mapping technique explores cancer cell mechanical nonlinearity that results from regional heterogeneity, which could help explain how metastatic cancer cells can show soft phenotypes while simultaneously increasing force generation and invasiveness.

1. Introduction

Measuring cell mechanical properties is important to better understand the arrangement of cellular structural networks associated with biological processes and disease pathogenesis (Bongiorno et al., 2014; Hu et al., 2020). Cellular compressive properties are frequently studied by treating the cell as a passive material and utilizing continuum mechanics models to determine the stiffness from force indentation curves (Humphrey, 2003; Ingber, 2003; Lim et al., 2006; Shin & Athanasiou, 1999; Unnikrishnan et al., 2007). The Hertzian contact mechanics model is most commonly used with atomic force microscopy (AFM) to determine cell stiffness (Johnson, 1985) simplifying cells as linearly elastic bodies undergoing small deformations (Radmacher et al., 1996; Suresh, 2007). However, cells may undergo large physiological deformations (Kc et al., 2006; Manimaran et al., 2006; Yamauchi et al., 2005) in which nonlinear models are more appropriate (D. X. Liu et al., 2010; Oommen & Van Vliet, 2006). In addition, cells are heterogeneous materials (Heidemann & Wirtz, 2004; Malandrino et al., 2018), which additionally contributes to nonlinear mechanical properties at large strains (Lammerding et al., 2007; Tseng et al., 2002). While various scanning probe mapping techniques have revealed the spatial variation in mechanical stiffness across individual cells (Darling, 2011; Fuhrmann et al., 2011; Raman et al., 2011) the effects of nonlinearity were not evaluated in these 2-D maps of elasticity. Conventional force mapping applies a prescribed value of force and records the cell deformation; the mechanical response may remain linear through the course of indentation at locations where the cell is thick (perinuclear region, e.g.), but not at locations where the cell is thin (lemellipodia, e.g.). Nonlinearity

* Corresponding author.
E-mail address: todd.sulchek@me.gatech.edu (T. Sulchek).
[1] Co-First Authors.

https://doi.org/10.1016/j.jbiomech.2023.111479
Accepted 30 January 2023
Available online 20 February 2023

resulting from significant deformation of the cell has been previously examined (Costa & Yin, 1999; Lin & Horkay, 2008; Zhang et al., 1997) and it was found that cell stiffness increases with large indentations. We have previously used the pointwise Hertzian approach (Costa et al., 2006) to determine the nonlinear response of elastomeric polydimethylsiloxane (PDMS) (Xu et al., 2011). Conventional force mapping utilizes the possibly nonlinear portions of force curves to extract Young's moduli, which can obfuscate the comparison of local material properties. We present a new technique called linear elastography that explicitly uses only the linear portion of the force curve (Fig. 1A) to determine a 2-D map of Young's modulus. We determine the linear elastography of cells by combining standard force mapping and the pointwise Hertzian method. This new technique systematically addresses the inherent nonlinearity of cellular mechanical measurements by finding and recording only the linear elasticity region for the purpose of stiffness mapping, which may reveal enhanced contrast of mechanical variations between cell regions.

Using this method, we found that the nominal strain marking the onset of nonlinear mechanical properties of the cell is region dependent. The linear elastography showed large spatial variations of mechanics with increased contrast of the nuclear region compared to that from conventional force mapping. The perinuclear regions of invasive ovarian and breast cancer cells were found to be softer than the surrounding cytoplasmic region. In contrast, less-invasive cancer cells did not show as high of a contrast between the lamellipodial and perinuclear stiffnesses. In the lamellipodia, the method found that cell stiffness is inversely correlated with local thickness for cells attached to the substrate. The elastography demonstrates the importance of spatial heterogeneity, cell morphology, and applied strain in determining cell mechanical properties. This technique may be particularly useful to examine the biomechanical changes to the perinuclear region of cells (Caille et al., 2002; Lammerding et al., 2007; Lombardi & Lammerding, 2010) in which realistic physiological strains characterize pathologies and processes, such as metastasis (Bissell et al., 1999; Friedl et al., 2011; Rowat et al., 2008; Zink et al., 2004).

2. Materials and methods

2.1. Atomic force microscopy and enhanced contrast microscopy

Atomic force microscopy (AFM) was conducted with the MFP-3D-Bio from Asylum Research. The AFM probe used was the C cantilever of MLCT (Bruker) with a nominal spring constant of 30 pN/nm modified with a plain silica bead of either 4.74 μm, 5.24 μm, or 7.32 μm in diameter attached to the cantilever tip with a two-part epoxy, which minimizes the lateral strain on the compressed cell. Prior to the force mapping, the AFM cantilever was calibrated on the glass bottom of a FluoroDish to determine the deflection inverse optical lever sensitivity. The cantilever was then raised away from the glass surface to monitor the thermal vibrations to assess the cantilever's spring constant using the thermal vibration method by fitting the thermal spectrum to a Lorentzian function. Ovarian and breast cancer cells were cultured overnight (see supplemental information) on the glass bottom of the FluoroDish prior to force mapping.

Measurements were conducted at room temperature (22–24 °C) and 20 % – 40 % relative humidity in RPMI-1640 cell media (Thermo Fisher). Enhanced contrast microscopy (Nikon) was used to visualize the general intracellular organization of cells during the measurements, as exemplified in Fig. 1B, in which the nucleus is visible under the microscope alongside the beaded indenter.

2.2. Linear elastography using pointwise Hertzian method and force mapping

Force mapping was conducted on 37 (9 HEY cells, 10 HEY A8 cells, 9 MCF10-A, 9 MCF10-CA) isolated single cells with one force map completed per cell. The scan area was chosen to include nucleus and the surrounding cytoplasmic region and typically ranged from 40 to 80 μm

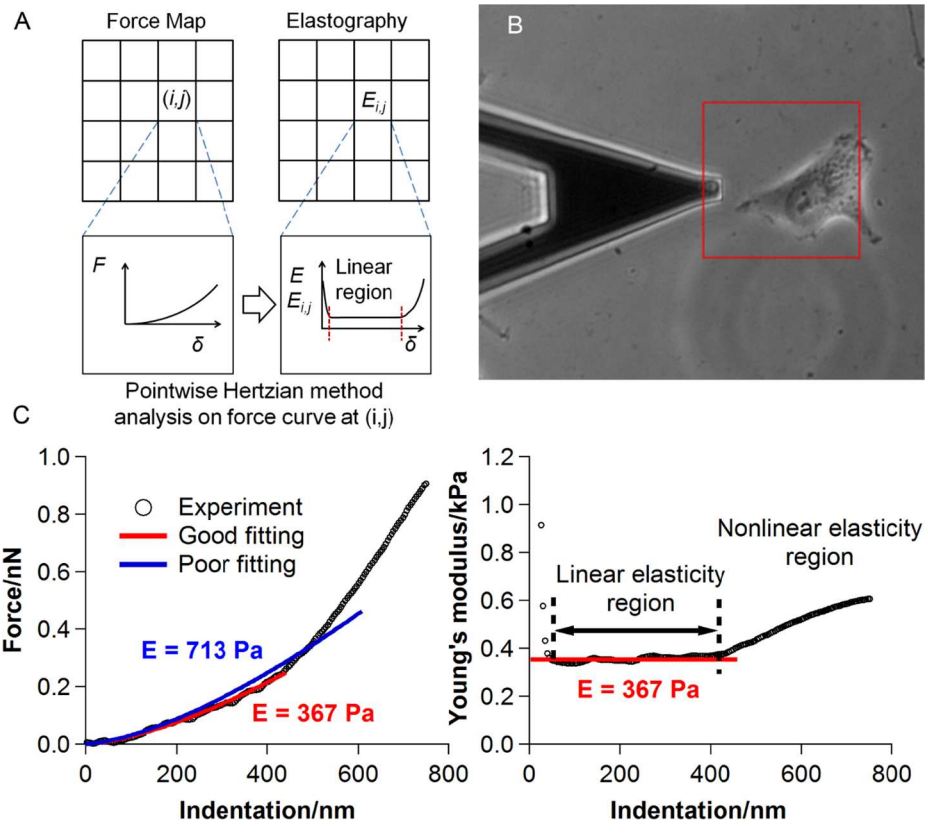

Fig. 1. Combination of enhanced contrast microscopy and linear elastography using pointwise Hertzian force mapping. A) A 2-D linear elastography map is generated from a 32 × 32 force map. In detail, force mapping measures force curves at equally distributed locations within the region of interest, which is then processed using the pointwise Hertzian method analysis on each force curve to determine the elasticity in the linear regime. Finally, we assemble the elastography map by identifying the linear region at each location and arranging the values into a 2-D matrix; B) Enhanced contrast microscopy visualizes the structural heterogeneity of single cells, where the nucleus is clearly visible; the scan region is 80 × 80 μm^2 as denoted by the red square; C) The mechanical properties of the single cells is highly nonlinear at large deformations, as indicated by Hertzian model fitting of the force curve when selecting different fit regions and pointwise Young's modulus versus indentation.

with a scan resolution ranging from 16 × 16 to 32 × 32. The approach and retraction velocity of the probe was set to 2 μm/s, while the XY scan velocity was set to 10 μm/s with a 0.5 s dwell away from the surface. The cell was indented until force from the cell was measured to be 5 nN. Overall, this resulted in a scan time of approximately 1–2 h per cell. The force curve at every pixel of the 2-D force map was analyzed using the pointwise Hertzian method (Costa et al., 2006; Xu et al., 2011) to evaluate the nonlinear mechanical behaviors during indentation. The average Young's modulus in the linear elasticity region was assembled into a 2-D matrix representing the linear elastography of the cell. The detailed procedures (with links to custom code repositories) are described in the supplemental information.

2.3. Finite element simulation of cell compression

Finite element simulation was employed to explore the effect of sample attachment upon the substrate on the mechanical response during deformation. A spherical indenter was used to indent the samples to a prescribed amount. Resultant force versus indentation curves were fit with the Hertzian model from 0 to 15 % nominal strain to calculate the Young's modulus. The simulation was implemented using Abaqus (SIMULIA Inc, Waltham, MA). The detailed procedures are described in the supplemental information.

2.4. Cellular structure imaging with confocal microscopy

The nucleus, actin cytoskeleton and plasma membrane of HEY A8 cells were stained following the procedures described in the supplemental information, and multiple images were acquired using a Zeiss LSM 510 NLO confocal microscope (Zeiss, Thornwood, NY). The z-stack function was also used to obtain the 3-D structural information of the nucleus, actin cytoskeleton and plasma membrane. The analysis was conducted upon single cells which were not in contact with other neighboring cells. The z-step was chosen to be 800 nm to ensure sufficient resolution with no layer of fluorescent actin or nucleus missed during the imaging.

2.5. Inhibition of Rho kinase by Y-27632

To evaluate the contribution of contractility to the pointwise modulus via the ROCK pathway, HEY A8 single cells treated with ROCK inhibitor Y-27632 (BD Biosciences, San Jose, CA) were measured. HEY A8 cells were incubated with 50 μM and 100 μM Y-27632 in cell culture media for 1 h at 37 ℃, and linear elastographies were obtained and compared with samples without treatment.

3. Results and discussion

3.1. Cells show nonlinear mechanical response under AFM indentation

Fitting an AFM force curve of a HEY A8 cell with the Hertzian contact model results in erroneous values of Young's modulus for a large fitting range (blue curve) (Fig. 1C). In the case of the reduced fitting range (red trace), a good quality fit is indicated by the overlap of fitting curve (red curve) with experimental curve, indicating a region of relatively constant pointwise Young's modulus. For the force curves examined, the Hertzian fitting is deficient due to nonlinear mechanics as the indentation exceeds 410 nm, though the exact deformation at which nonlinearity emerges can vary. We therefore identify linear and nonlinear regions in the pointwise Young's modulus curve, consistent with previous studies of biomaterials (Costa et al., 2006; Mahaffy et al., 2004) (Fig. 1C).

3.2. Linear elastography mapping reveals spatial variation of cell mechanical properties

Following the methods described above, linear elastography reveals spatial variation of cell stiffness for the HEY A8, HEY, MCF10-CA and MCF10-A cell types (Fig. 2), including regions of increased stiffness in the cytoskeletal region and with significantly softer perinuclear regions in the case of metastatic cell types. At a population level, HEY A8 ovarian cancer cells have been identified as softer and more migratory than their HEY counterparts (Xu et al., 2012). Similarly, MCF10-CA breast cancer cells are the more metastatic derivative of the MCF10-A parent cell line which have been shown to migrate in a more coordinated manner (Santner et al., 2001, Aaltonen et al., 2022). Force-indentation curves measured at the cell surface with atomic force microscopy reflect the underlying cell structure and because of the coupling of the nucleus and intracellular actin structures to the cell surface, indentations translate into compression of all components underneath the probe (Haase & Pelling, 2015; Mathur et al., 2001). We therefore infer that heterogenous mechanical properties measured across the cell are due to heterogeneity of cell internal structures, for example F-actin bundles.

The elastographies after surface correction (Figure S1) display enhanced contrast of spatial variations and indicate that mechanical stiffness of cells can be highly heterogeneous along lateral dimensions, especially compared to fixed force trigger force mapping (Figure S2). The central region corresponding to the nucleus shows lower Young's moduli than the cytoplasm. The cytoplasmic region surrounding the nucleus was seen to have higher moduli than the perinuclear region for the invasive HEY A8 cells but not for less invasive HEY cells (Fig. 2). The elastographies of the MCF10 cell line display a softer perinuclear region relative to the lamellipodia region in the invasive MCF10-CA cells when compared to the less-invasive MCF10-A cells (Figure S3).

3.3. Confocal microscopy reveals the structural contribution of nucleus and cytoplasm

From these results, we find the Young's modulus across the perinuclear region is lower than the moduli in the lamellipodia region for both metastatic ovarian and breast cancer types based on a comparison of four cell lines representing invasive and less invasive ovarian (HEY A8 vs HEY) and breast (MCF10CA vs MCF10A) cancer cell types. While the difference in stiffness is consistent with the spatial variation of cellular structures shown in Fig. 3, it remains unclear to what degree the nucleus contributes to the local stiffness since the nucleus and cytoskeletal structures are colocalized at each pixel and each will contribute to the measured mechanical properties. We therefore determined the fraction of the cellular space occupied by the nucleus and cytoplasm through staining and confocal microscopy of the actin cytoskeleton, nucleus, and plasma membrane of individual cells. From these images, the 2-D side view projection and representative images of the nucleus, actin cytoskeleton, and plasma membrane were obtained (Fig. 3).

From the 2-D projection of the cellular structure of the HEY A8 cells, the actin cytoskeleton stress fibers are clearly visible and thinly spread over the extended cytoplasm and the nucleus is a flattened ellipse. From the side view, the nucleus fills most of the cell body, with only a thin region of F-actin cytoskeletal below the nucleus. The cellular thickness and nuclear extent observed in confocal images are consistent with that observed in AFM topography and elastography. From Fig. 3E-H, the cell body over the nuclear region is primarily occupied by the nucleus. Therefore, we conclude that the mechanics over the nuclear region are dominated by deformation of the nucleus. Thus, the central, circular cellular regions of soft elastography measurements primarily reflect the softness of the nucleus for the indentation depths much larger than the thickness of the cytoskeletal layer. The elastography, together with the confocal microscopy and phase contrast images, showed that the nucleus is softer than the surrounding cytoplasm in HEY A8 cells when

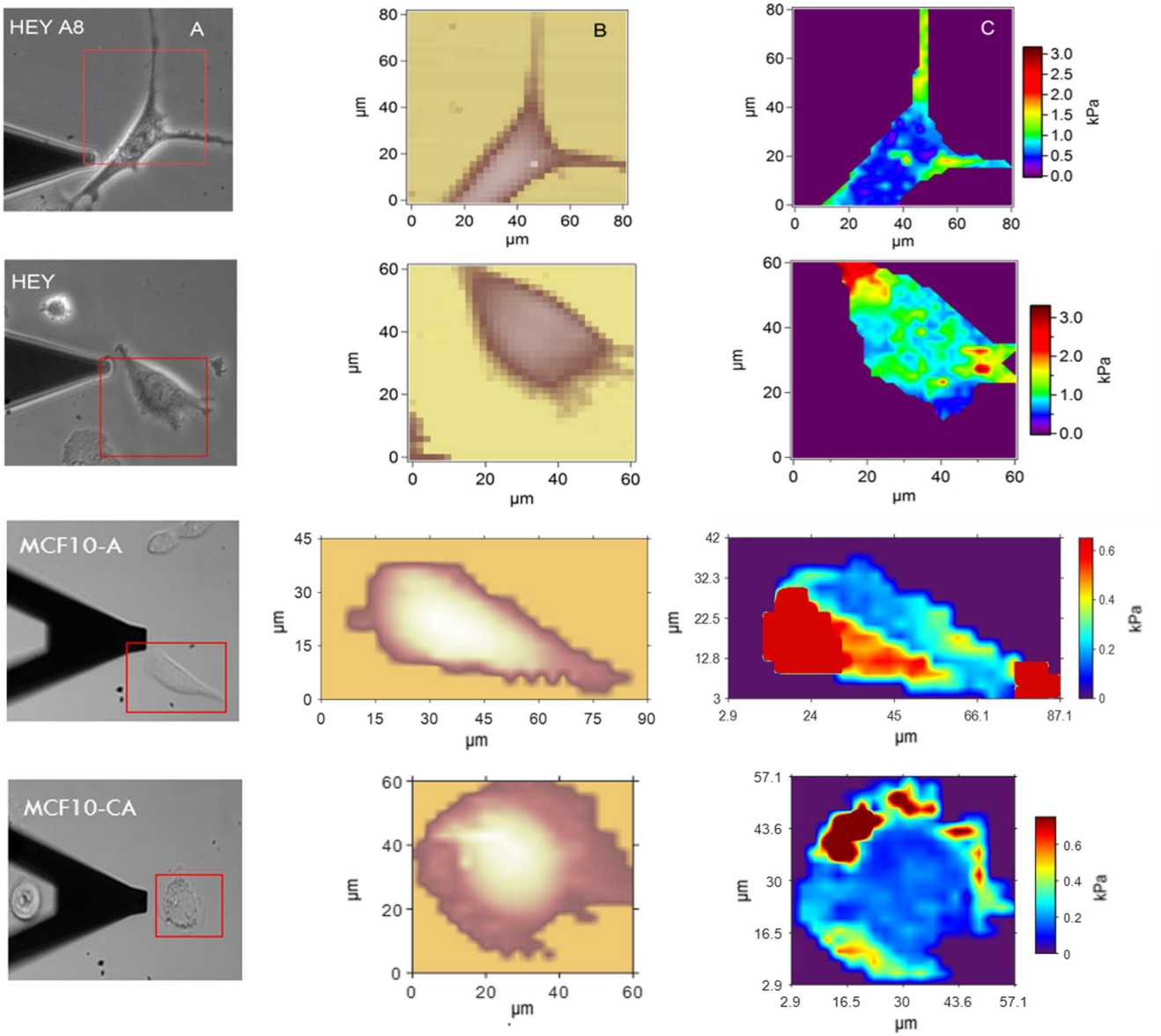

Fig. 2. Images and linear elastographies of ovarian cancer cell lines (HEY A8, HEY), and breast cancer cell lines (MCF10-A, MCF10-CA). A) Enhanced contrast microscopy shows the cell boundary and edge of the nucleus. B) The region defined by the red box was scanned to show a 2-D representation of the topography. C) The corresponding elastographies show linear elasticity distribution of the cells, in which the nuclear region is softer than the surrounding cytoplasm in invasive HEYA8 and MCF10-CA cells. In contrast, noninvasive cancer cells from HEY and MCF10-A do not show a softer nuclear region.

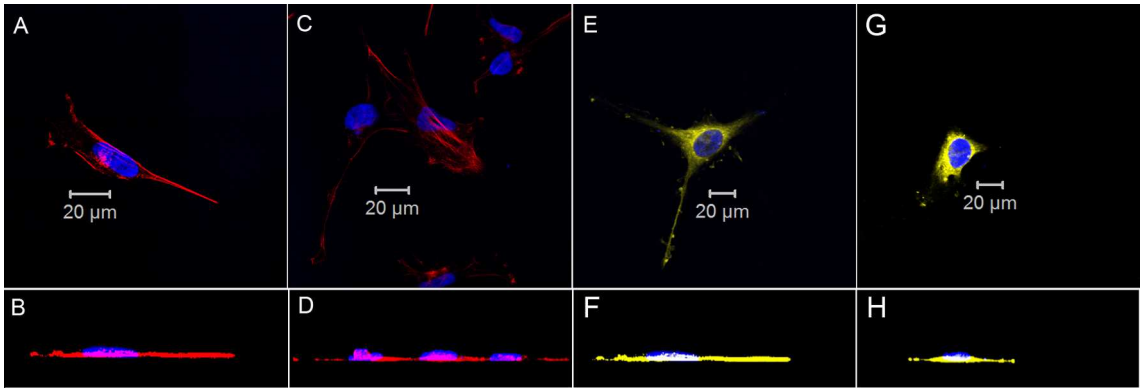

Fig. 3. Confocal microscopy displays nucleus (blue), F-actin (red) and plasma membrane (yellow) of HEY A8 cells, A-D) nucleus and F-actin staining, E-H: nucleus and plasma membrane staining. Top row: top view of single cells and cell clusters; bottom row: side view of corresponding cells and cell clusters. It is seen that the nucleus contributes to most of the volume in the perinuclear region of adherent HEY A8 cells.

material strain is considered (see supplemental information). We observe that the difference in mechanics of the perinuclear and lamellipodia is more apparent for the comparison between metastatic and less metastatic cells. Differences in subcellular mechanics can still be seen in the nonlinear regime (i.e. high strain), however. Therefore, cells that experience nonlinear strain may still be limited by nuclear deformation.

The fact that the nucleus of invasive HEY A8 and MCF10-CA cell types is at least as soft as the surrounding cytoplasm is consistent with the role of the nucleus as a key limiting factor in cancer cell migration (Friedl et al., 2011; Fu et al., 2012). The nuclei in cancer cells can display a ruptured and less organized structure (Zink et al., 2004) resulting in a decreased mechanical stiffness that associates with altered structure of nuclei in cancer cells. Since the deformation of the nucleus is a critical step in cell transport in physiological scenarios, and possibly the rate-limiting factor (Beadle et al., 2008; Schoumacher et al., 2010; Wolf et al., 2007) of cancer cell migration (Fu et al., 2012; Yamauchi et al., 2005), cells with more deformable nuclei more easily migrate through small confines and are thus more invasive.

3.4. Young's modulus in the lamellipodia region reveals a dramatic thickness-dependence

The high-resolution measurement of the modulus of the lamellipodia of the HEY A8 cell (Fig. 4A) reveals an inverse relationship with cell thickness such that thinner regions are stiffer. To quantitatively explore the correlation, the Young's modulus versus thickness at different locations is plotted in Fig. 4B. As the indenter diameter is substantially larger than the pixel size (1.875 μm), pixels at the cell boundary were not included in the analysis. We observed two different topographical regions that both show strong correlation between stiffness and cell thickness that follow exponential relationships. Specific contributions to the exponential relationship that results from the geometrically confined system were further examined.

3.5. Contractility contributes to stiffness but not the exponential dependence on cell thickness

Having established the correlation between stiffness and cell thickness and demonstrated strong spatial variations in elasticity in lamellipodia of HEY A8 cells which vary by more than 2 kPa, we further investigated conditions that affect the exponential dependence on cell thickness. While several biological factors might contribute to the stiffening observed in the lamellar region, we also explore a purely mechanical explanation in this relation (Xu et al., 2011). We hypothesize that contractility may affect the exponential dependence between stiffness and cell thickness, as it is also known to contribute to variations of stiffness in cells (Chernaya et al., 2018; Nagayama et al., 2004; Vichare et al., 2012; Wang et al., 2002). Variations of contractility, particularly in lamellipodia where the cytoskeletal structures form the bulk of the volume (Butler et al., 2002; Nagayama et al., 2004; Wang et al., 2002), may also result in distinct relationships between the stiffness and the cell thickness. To evaluate the relative contribution of contractility on the observed exponential relationship, we decreased cytoskeletal tension using a chemical treatment, and monitored the effect on thickness-dependent cell stiffness. ROCK inhibitor Y-27632 was added to inhibit the actomyosin contractility *via* Rho pathway, and subsequent AFM stiffness measurements were conducted (Fig. 5A). Inhibition of actomyosin contractility subsequently reduced the stiffness of HEY A8 cells. Increasing the concentration of Y-27632 from 50 μM to 100 μM does not further reduce the stiffness of HEY A8 cells (Figure S4). Upon inhibition, the stiffness of HEY A8 cells in the cytoplasmic region decreased by 50 % to 1.3 kPa. The stiffness of the nuclear region, in contrast, did not undergo appreciable changes, supporting our conclusion that cytoplasmic F-actin contractility contributes little to the measured perinuclear stiffness. As a result, the nuclei are not distinguishable in the elastographies of HEY A8 cells treated with Y-27632, implying the strong contribution of actomyosin contractility to cellular stiffness in the cytoplasmic region, but not to the perinuclear region. This observation was particularly interesting in the light of other studies that have demonstrated the coupling of the actin cytoskeleton in the cytoplasm and nuclear structure (Mazumder et al., 2010). By inhibiting ROCK and affecting actomyosin contractility, we could also be releasing the tension on a pre-stressed nucleus which may also result in nuclear softening. Based on our measurements, we hypothesize that the decrease in stiffness observed in studies of invasive cells (Alibert et al., 2017; Fischer et al., 2017; Luo et al., 2016), is primarily a result of perinuclear softening (Deville & Cordes, 2019), and not due to cytoplasmic softening. This observation is consistent with studies showing that invasive cells are capable of significant force generation and increased contractility (Kraning-Rush et al., 2012; Mekhdjian et al., 2017b; Mierke et al., 2011), typically associated with cell stiffening, while also possessing more deformable nuclei (Mekhdjian et al., 2017a). This difference in global and local cell stiffness could potentially be explained by changes in the composition and spatial organization of the cytoskeleton to allow for decreased resistance to cell movement and increased force generation (Alibert et al., 2020). It is known that contraction force, sometimes called prestress, increases the stiffness of single cells (Vichare et al., 2012; Wang et al., 2002). The distribution pattern of Young's modulus in the cortical region in our experiment is similar to that of contraction force field exerted by other cell types (Butler et al., 2002).

After inhibition of actomyosin contractility, linear elastography was obtained over an area of 30 × 30 μm^2 in the lamellipodia. The resultant modulus was plotted against local thickness in Fig. 5B, along with the scanned topography. Even with the contractile stress inhibited, the exponential dependence on local cell thickness emerges. Therefore, actomyosin prestress provides an important contribution to cellular

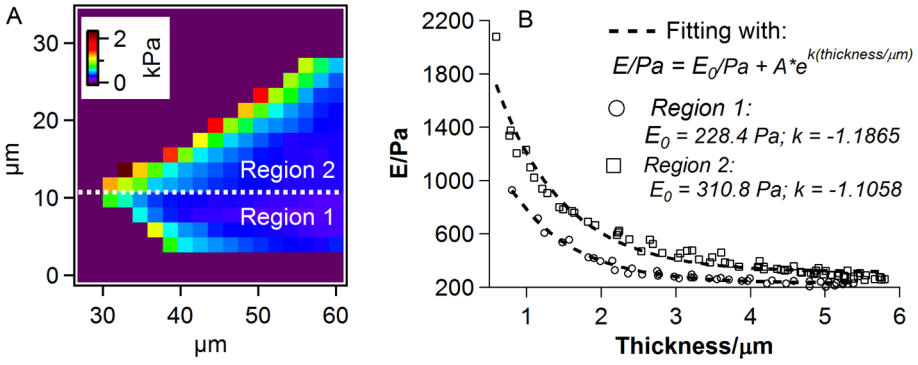

Fig. 4. Linear elastography versus local cell thickness over a lamellipodia of a HEY A8 cell. A) A linear elastography map for a representative HEY A8 cell lamellipodia region is shown. A white dashed line separates two regions of interest. B) Elastography values for Region 1 and Region 2 are plotted versus the measured cell thickness. A fit of exponential law curves is shown for the two regions.

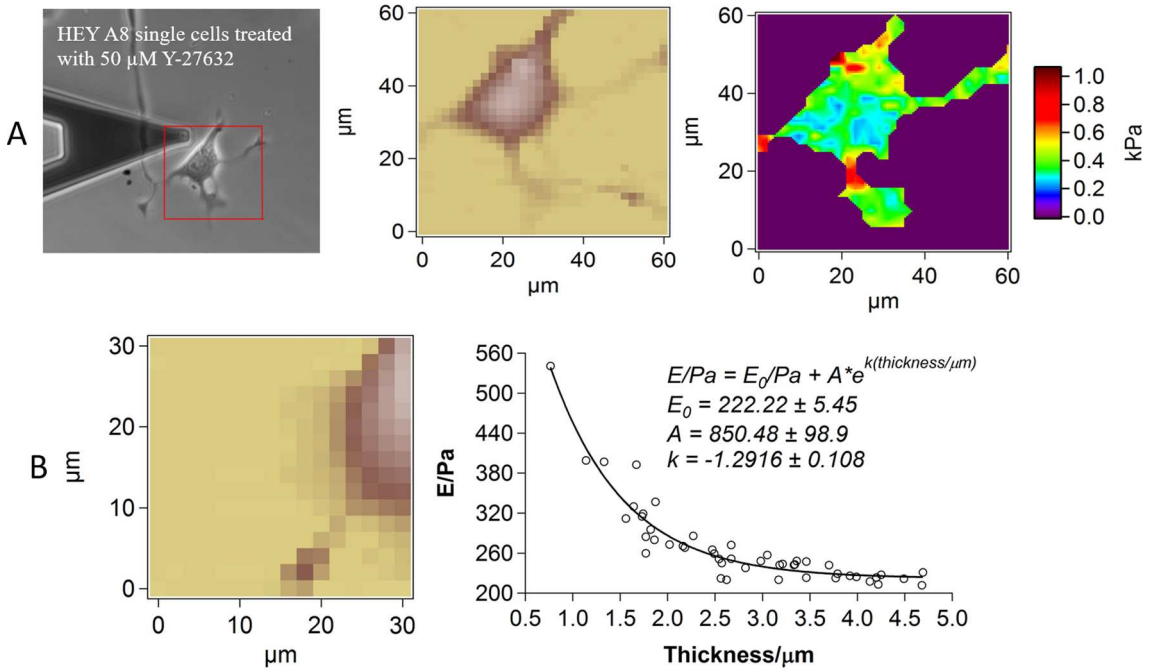

Fig. 5. Elastographies of HEY A8 single cells treated with 50 μM Y-27632: A) enhanced contrast images, topography, and stiffness map. B) Linear elastography versus thickness for the cell edge. The stiffness depends exponentially on thickness even after chemical softening.

stiffness, but it does not account for the dependence of stiffness on cell thickness.

3.6. *Finite element simulation reveals the exponential dependence of stiffness on cell thickness results from cell attachment to the substrate*

Figs. 4 and 5B demonstrate a dramatic stiffening phenomenon in which linear elasticity strongly depends on local cell thickness. Similar thickness-dependent stiffening was observed in a variety of polymer materials (Akhremitchev & Walker, 1999; Ao & Li, 2011; M. Liu et al., 2009; Oommen & Van Vliet, 2006), indicating the effect may be more purely mechanical in nature. We hypothesize that this stiffening is a result of the confinement and restriction of the lateral movement of the material during compression that results from attachment of the cell to the underlying stiff substrate. The boundary condition of zero displacements imposed by the substrate implies the material displacement is more constrained at any location as compared to when material is not bonded to a stiff substrate. As the cell thickness decreases, the effect is more pronounced as the ratio of interface to regional volume increases. Finite element simulation was employed to test this hypothesis (Fig. 6). The bonded sample has a higher peak stress than the unbonded sample for the same amount of indentation. Additionally, the Young's modulus of the bonded sample shows a strong exponential dependence on thickness; in contrast, the unbonded sample shows no variation of Young's modulus with sample thickness, for the entirety of thicknesses examined. The stiffening in finite element simulation closely supports the experimental cell data observed in Fig. 5B, and points to an explanation of the observed stiffening. The effect of attachment on mechanical response gradually decreases with increasing sample thickness—at 6 μm, the calculated Young's modulus approaches the predefined value of 600 Pa, suggesting that the effect of attachment on linear elasticity in the center of the cell is negligible.

Our studies of the lamellipodia region of HEY A8 cells and previously studied polymers (Xu et al., 2011), together with the finite element simulation, revealed that linear elasticity maps at small indentations are affected by cell attachment, as compared to other experiments (Akhremitchev & Walker, 1999; Dimitriadis et al., 2002; Kovalev et al., 2004;

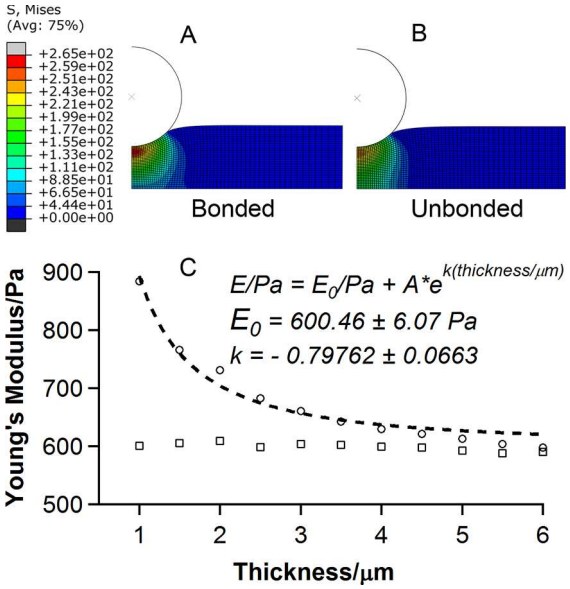

Fig. 6. Finite element simulation reveals the effect of bonding between substrate and sample on mechanical response. A) Image of FEA model of a sample bonded to the substrate, B) Image of FEA model of a sample unbonded to the substrate, and C) Resultant Young's modulus versus thickness for bonded (represented by circles) and unbonded (represented by squares) samples.

M. Liu et al., 2009; Santos et al., 2012) and theoretical models (Chadwick, 2002; Dhaliwal, 1970; Hayes et al., 1972; Sneddon, 1951, 1965) which only show the impact of finite sample thickness on mechanical response. Moreover, the study addressed the importance of considering constraints in the evaluation of mechanical behavior at the nano/micro scale, in which the stiffening might be significant compared to bulk material. Our model assumes strong adhesion between the cell and substrate, which constrains the deformation of the cell elements. One could imagine for weakly adherent cells, sliding may be possible

reducing the effective modulus. We should also note these measurements were performed at ambient temperature, which may influence distinct cell behaviors from physiological temperature.

4. Summary and conclusion

In this paper, we described the combination of pointwise Hertzian method and standard force mapping with AFM to obtain elastography of single cells and demonstrated that the linear elasticity of these cells can be utilized to map underlying internal structures with greater resolution. We observed the nucleus is much softer than the surrounding cytoplasm in the invasive HEY A8 and MCF10-CA cancer cells, but not in the less invasive HEY and MCF10-A cells. In addition, there exists a strong stiffening phenomenon at the lamellipodia, with stiffness depending on local thickness with an exponential relationship. The correlation between elasticity and sample thickness still exists after inhibition of actomyosin contractility. Finite element simulation revealed that the stiffening is due to the bonding of cell upon substrate, suggesting the important role of sample bonding in stiffness measurement. Together, the observation from the novel method suggests an answer to the paradox of motile cancer cell softening while demonstrating increased contractility and traction force (Alibert et al., 2017; Nguyen et al., 2016).

The results shown here demonstrated the capability of the pointwise Hertzian method in cell mechanics study with AFM, the heterogeneity of mechanical properties could be difficult to detect otherwise. The application of this systematic approach to metastatic HEY A8 and MCF10-CA cells revealed the softening of the nuclear region, and additionally, the mechanical stiffening at the cell lamellipodia suggested the significance of cell-substrate interactions in cell mechanics measurements, which might become more significant as confinement reaches to smaller scales.

Significance Statement.

This work describes a new cell force mapping technique that accounts for variations in applied strain, local thickness, and cell surface curvature to reveal mechanical contrast. The method allows for distinct visualization of the nucleus and cytoplasm by considering the nonlinearity of cell mechanical properties. We observe that invasive cancer cells can have significantly softer nuclear regions compared to their lamellipodial regions, which may help explain how metastatic cancer cells can present softer phenotypes while simultaneously generating higher forces and motility. We also show that cells stiffen in direct relation to their confinement by the underlying substrate. This technique could be useful to investigate the mechanical properties of other cancer cells, immune cells, and cell types capable of motility and force generation.

CRediT authorship contribution statement

Wenwei Xu: Writing – original draft, Visualization, Software, Methodology, Investigation, Formal analysis, Conceptualization. **Saif Kabariti:** Writing – review & editing, Visualization, Validation, Software, Methodology, Formal analysis. **Katherine M. Young:** Writing – review & editing, Visualization, Validation, Software, Investigation, Formal analysis. **Steven P. Swingle:** Formal analysis, Methodology, Validation. **Alan Y. Liu:** Formal analysis, Methodology, Validation. **Todd Sulchek:** Writing – review & editing, Supervision, Project administration, Funding acquisition, Conceptualization.

Declaration of Competing Interest

The authors declare that they have no known competing financial interests or personal relationships that could have appeared to influence the work reported in this paper.

Acknowledgments

The authors gratefully acknowledge John McDonald and Roman Mezencev for providing guidance on cell culture and other valuable advice. Funding was provided by the National Science Foundation, Grant # CBET-2225476, as well as National Institutes of Health Grant # R01GM144727. The funders had no role in study design, data collection and analysis, decision to publish, or preparation of the manuscript.

Appendix A. Supplementary material

Supplementary data to this article can be found online at https://doi.org/10.1016/j.jbiomech.2023.111479.

References

Aaltonen, N., Kyykallio, H., Tollis, S., Capra, J., Hartikainen, J.M., Matilainen, J., Oikari, S., Rilla, K., 2022. MCF10CA Breast Cancer Cells Utilize Hyaluronan-Coated EV-Rich Trails for Coordinated Migration. Front. Oncol. 12, 869417 https://doi.org/10.3389/fonc.2022.869417.

Akhremitchev, B.B., Walker, G.C., 1999. Finite sample thickness effects on elasticity determination using atomic force microscopy. Langmuir 15 (17), 5630–5634. https://doi.org/10.1021/la980585z.

Alibert, C., Pereira, D., Lardier, N., Etienne-Manneville, S., Goud, B., Asnacios, A., & Manneville, J.-B. 2020 Intracellular stiffening competes with cortical softening in glioblastoma cells. *BioRxiv*, 2020.09.02.279794. https://doi.org/10.1101/2020.09.02.279794.

Alibert, C., Goud, B., Manneville, J.-B., 2017. Are cancer cells really softer than normal cells? Biol. Cell 109 (5), 167–189. https://doi.org/10.1111/boc.201600078.

Ao, Z., Li, S., 2011. Temperature- and thickness-dependent elastic moduli of polymer thin films. Nanoscale Res. Lett. 6 (1), 243. https://doi.org/10.1186/1556-276X-6-243.

Beadle, C., Assanah, M.C., Monzo, P., Vallee, R., Rosenfeld, S.S., Canoll, P., 2008. The role of myosin II in glioma invasion of the brain. Mol. Biol. Cell 19 (8), 3357–3368. https://doi.org/10.1091/mbc.e08-03-0319.

Bissell, M.J., Weaver, V.M., Lelièvre, S.A., Wang, F., Petersen, O.W., Schmeichel, K.L., 1999. Tissue structure, nuclear organization, and gene expression in normal and malignant breast. Cancer Res. 59 (7), 1757s–1764s.

Bongiorno, T., Kazlow, J., Mezencev, R., Griffiths, S., Olivares-Navarrete, R., McDonald, J.F., Schwartz, Z., Boyan, B.D., McDevitt, T.C., Sulchek, T., 2014. Mechanical stiffness as an improved single-cell indicator of osteoblastic human mesenchymal stem cell differentiation. J. Biomech. 47 (9), 2197–2204. https://doi.org/10.1016/j.jbiomech.2013.11.017.

Butler, J.P., Tolić-Nørrelykke, I.M., Fabry, B., Fredberg, J.J., 2002. Traction fields, moments, and strain energy that cells exert on their surroundings. Am. J. Physiol. Cell Physiol. 282 (3), C595–C605. https://doi.org/10.1152/ajpcell.00270.2001.

Caille, N., Thoumine, O., Tardy, Y., Meister, J.-J., 2002. Contribution of the nucleus to the mechanical properties of endothelial cells. J. Biomech. 35 (2), 177–187. https://doi.org/10.1016/s0021-9290(01)00201-9.

Chadwick, R. S. 2002. Axisymmetric indentation of a thin incompressible elastic layer. *SIAM Journal on Applied Mathematics*, *62*(5), 1520–1530. Scopus. https://doi.org/10.1137/S0036139901388222.

Chernaya, O., Zhurikhina, A., Hladyshau, S., Pilcher, W., Young, K.M., Ortner, J., Andra, V., Sulchek, T.A., Tsygankov, D., 2018. Biomechanics of endothelial tubule formation differentially modulated by cerebral cavernous malformation proteins. IScience 9, 347–358. https://doi.org/10.1016/j.isci.2018.11.001.

Costa, K.D., Sim, A.J., Yin, F.-C.-P., 2006. Non-Hertzian approach to analyzing mechanical properties of endothelial cells probed by atomic force microscopy. J. Biomech. Eng. 128 (2), 176–184. https://doi.org/10.1115/1.2165690.

Costa, K.D., Yin, F.C., 1999. Analysis of indentation: Implications for measuring mechanical properties with atomic force microscopy. J. Biomech. Eng. 121 (5), 462–471. https://doi.org/10.1115/1.2835074.

Darling, E.M., 2011. Force scanning: a rapid, high-resolution approach for spatial mechanical property mapping. Nanotechnology 22 (17), 175707. https://doi.org/10.1088/0957-4484/22/17/175707.

Deville, S.S., Cordes, N., 2019. The Extracellular, Cellular, and Nuclear Stiffness, a Trinity in the Cancer Resistome-A Review. Front. Oncol. 9, 1376. https://doi.org/10.3389/fonc.2019.01376.

Dhaliwal, R.S., 1970. Punch problem for an elastic layer overlying an elastic foundation. Int. J. Eng. Sci. 8 (4), 273–288. https://doi.org/10.1016/0020-7225(70)90058-3.

Dimitriadis, E.K., Horkay, F., Maresca, J., Kachar, B., Chadwick, R.S., 2002. Determination of elastic moduli of thin layers of soft material using the atomic force microscope. Biophys. J . 82 (5), 2798–2810. https://doi.org/10.1016/S0006-3495(02)75620-8.

Fischer, T., Wilharm, N., Hayn, A., Mierke, C.T., 2017. Matrix and cellular mechanical properties are the driving factors for facilitating human cancer cell motility into 3D engineered matrices. Convergent Sci. Phys. Oncol. 3 (4), 044003 https://doi.org/10.1088/2057-1739/aa8bbb.

Friedl, P., Wolf, K., Lammerding, J., 2011. Nuclear mechanics during cell migration. Curr. Opin. Cell Biol. 23 (1), 55–64. https://doi.org/10.1016/j.ceb.2010.10.015.

Fu, Y., Chin, L.K., Bourouina, T., Liu, A.Q., VanDongen, A.M.J., 2012. Nuclear deformation during breast cancer cell transmigration. Lab Chip 12 (19), 3774–3778. https://doi.org/10.1039/c2lc40477j.

Fuhrmann, A., Staunton, J.R., Nandakumar, V., Banyai, N., Davies, P.C.W., Ros, R., 2011. AFM stiffness nanotomography of normal, metaplastic and dysplastic human esophageal cells. Phys. Biol. 8 (1), 015007 https://doi.org/10.1088/1478-3975/8/1/015007.

Haase, K., Pelling, A.E., 2015. Investigating cell mechanics with atomic force microscopy. J. R. Soc. Interface 12 (104), 20140970. https://doi.org/10.1098/rsif.2014.0970.

Hayes, W.C., Keer, L.M., Herrmann, G., Mockros, L.F., 1972. A mathematical analysis for indentation tests of articular cartilage. J. Biomech. 5 (5), 541–551. https://doi.org/10.1016/0021-9290(72)90010-3.

Heidemann, S.R., Wirtz, D., 2004. Towards a regional approach to cell mechanics. Trends Cell Biol. 14 (4), 160–166. https://doi.org/10.1016/j.tcb.2004.02.003.

Hu, L., Ni, F., Wang, X., Fay, M.E., Young, K.M., Lam, W.A., Sulchek, T.A., Qu, C.-K., 2020. Decreased cell stiffness enhances leukemia development and progression. Leukemia 34 (9), 2493–2497. https://doi.org/10.1038/s41375-020-0763-7.

Humphrey, J. d. 2003 Review Paper: Continuum biomechanics of soft biological tissues. *Proceedings of the Royal Society of London. Series A: Mathematical, Physical and Engineering Sciences*, *459*(2029), 3–46. https://doi.org/10.1098/rspa.2002.1060.

Ingber, D.E., 2003. Tensegrity I. cell structure and hierarchical systems biology. J. Cell Sci. 116 (7), 1157–1173. https://doi.org/10.1242/jcs.00359.

Johnson, K.L., 1985. Contact Mechanics. Cambridge University Press. https://doi.org/10.1017/CBO9781139171731.

Kc, C., M, M., Fe, T., S, S., 2006. A quantitative observation and imaging of single tumor cell migration and deformation using a multi-gap microfluidic device representing the blood vessel. Microvasc. Res. 72 (3), 153–160. https://doi.org/10.1016/j.mvr.2006.06.003.

Kovalev, A., Shulha, H., Lemieux, M., Myshkin, N., Tsukruk, V.V., 2004. Nanomechanical Probing of Layered Nanoscale Polymer Films With Atomic Force Microscopy. J. Mater. Res. 19 (3), 716–728. https://doi.org/10.1557/jmr.2004.19.3.716.

Kraning-Rush, C.M., Califano, J.P., Reinhart-King, C.A., 2012. Cellular traction stresses increase with increasing metastatic potential. PLoS One 7 (2), e32572.

Lammerding, J., Dahl, K.N., Discher, D.E., Kamm, R.D., 2007. Nuclear mechanics and methods. Methods Cell Biol. 83, 269–294. https://doi.org/10.1016/S0091-679X(07)83011-1.

Lim, C.T., Zhou, E.H., Quek, S.T., 2006. Mechanical models for living cells—a review. J. Biomech. 39 (2), 195–216. https://doi.org/10.1016/j.jbiomech.2004.12.008.

Lin, D.C., Horkay, F., 2008. Nanomechanics of polymer gels and biological tissues: a critical review of analytical approaches in the Hertzian regime and beyond. Soft Matter 4 (4), 669–682. https://doi.org/10.1039/B714637J.

Liu, M., Sun, J., Sun, Y., Bock, C., Chen, Q., 2009. Thickness-dependent mechanical properties of polydimethylsiloxane membranes. J. Micromech. Microeng. 19, 035028 https://doi.org/10.1088/0960-1317/19/3/035028.

Liu, D.X., Zhang, Z.D., Sun, L.Z., 2010. Nonlinear elastic load–displacement relation for spherical indentation on rubberlike materials. J. Mater. Res. 25 (11), 2197–2202. https://doi.org/10.1557/jmr.2010.0285.

Lombardi, M.L., Lammerding, J., 2010. Altered mechanical properties of the nucleus in disease. Methods Cell Biol. 98, 121–141. https://doi.org/10.1016/S0091-679X(10)98006-0.

Luo, Q., Kuang, D., Zhang, B., Song, G., 2016. Cell stiffness determined by atomic force microscopy and its correlation with cell motility. BBA 1860 (9), 1953–1960. https://doi.org/10.1016/j.bbagen.2016.06.010.

Mahaffy, R.E., Park, S., Gerde, E., Käs, J., Shih, C.K., 2004. Quantitative analysis of the viscoelastic properties of thin regions of fibroblasts using atomic force microscopy. Biophys. J . 86 (3), 1777–1793. https://doi.org/10.1016/S0006-3495(04)74245-9.

Malandrino, A., Mak, M., Kamm, R.D., Moeendarbary, E., 2018. Complex mechanics of the heterogeneous extracellular matrix in cancer. Extreme Mech. Lett. 21, 25–34. https://doi.org/10.1016/j.eml.2018.02.003.

Manimaran, M., Tay, F.E.H., Chaw, K.C., 2006. Cell Deformation in Cancer Metastasis: a BioMEMS Based Approach. J. Phys. Conf. Ser. 34, 1143–1147. https://doi.org/10.1088/1742-6596/34/1/189.

Mathur, A.B., Collinsworth, A.M., Reichert, W.M., Kraus, W.E., Truskey, G.A., 2001. Endothelial, cardiac muscle and skeletal muscle exhibit different viscous and elastic properties as determined by atomic force microscopy. J. Biomech. 34 (12), 1545–1553. https://doi.org/10.1016/S0021-9290(01)00149-X.

Mazumder, A., Shivashankar, G.V., 2010. Emergence of a prestressed eukaryotic nucleus during cellular differentiation and development. J. R. Soc. Interface 7, S321–S330. https://doi.org/10.1098/rsif.2010.0039.focus.

Mekhdjian, A.H., Kai, F., Rubashkin, M.G., Prahl, L.S., Przybyla, L.M., McGregor, A.L., Bell, E.S., Barnes, J.M., DuFort, C.C., Ou, G., Chang, A.C., Cassereau, L., Tan, S.J., Pickup, M.W., Lakins, J.N., Ye, X., Davidson, M.W., Lammerding, J., Odde, D.J., Weaver, V.M., 2017. Integrin-mediated traction force enhances paxillin molecular associations and adhesion dynamics that increase the invasiveness of tumor cells into a three-dimensional extracellular matrix. Mol. Biol. Cell 28 (11), 1467–1488. https://doi.org/10.1091/mbc.e16-09-0654.

Mierke, C.T., Frey, B., Fellner, M., Herrmann, M., Fabry, B., 2011. Integrin α5β1 facilitates cancer cell invasion through enhanced contractile forces. J. Cell Sci. 124 (Pt 3), 369–383. https://doi.org/10.1242/jcs.071985.

Nagayama, M., Haga, H., Takahashi, M., Saitoh, T., Kawabata, K., 2004. Contribution of cellular contractility to spatial and temporal variations in cellular stiffness. Exp. Cell Res. 300 (2), 396–405. https://doi.org/10.1016/j.yexcr.2004.07.034.

Nguyen, A.V., Nyberg, K.D., Scott, M.B., Welsh, A.M., Nguyen, A.H., Wu, N., Hohlbauch, S.V., Geisse, N.A., Gibb, E.A., Robertson, A.G., Donahue, T.R., Rowat, A. C., 2016. Stiffness of pancreatic cancer cells is associated with increased invasive potential. Integr. Biol. 8 (12), 1232–1245. https://doi.org/10.1039/c6ib00135a.

Oommen, B., Van Vliet, K.J., 2006. Effects of nanoscale thickness and elastic nonlinearity on measured mechanical properties of polymeric films. Thin Solid Films 513 (1), 235–242. https://doi.org/10.1016/j.tsf.2006.01.069.

Radmacher, M., Fritz, M., Kacher, C.M., Cleveland, J.P., Hansma, P.K., 1996. Measuring the viscoelastic properties of human platelets with the atomic force microscope. Biophys. J . 70 (1), 556–567.

Raman, A., Trigueros, S., Cartagena, A., Stevenson, A.P.Z., Susilo, M., Nauman, E., Contera, S.A., 2011. Mapping nanomechanical properties of live cells using multi-harmonic atomic force microscopy. Nat. Nanotechnol. 6 (12), 809–814. https://doi.org/10.1038/nnano.2011.186.

Rowat, A.C., Lammerding, J., Herrmann, H., Aebi, U., 2008. Towards an integrated understanding of the structure and mechanics of the cell nucleus. Bioessays 30 (3), 226–236. https://doi.org/10.1002/bies.20720.

Santner, S.J., Dawson, P.J., Tait, L., Soule, H.D., Eliason, J., Mohamed, A.N., Wolman, S. R., Heppner, G.H., Miller, F.R., 2001. Malignant MCF10CA1 cell lines derived from premalignant human breast epithelial MCF10AT cells. Breast Cancer Res. Treat. 65 (2), 101–110. https://doi.org/10.1023/a:1006461422273.

Santos, J.a. C., Rebêlo, L.M., Araujo, A.C., Barros, E.B., Sousa, J.S.de., 2012. Thickness-corrected model for nanoindentation of thin films with conical indenters. Soft Matter 8 (16), 4441–4448. https://doi.org/10.1039/C2SM07062F.

Schoumacher, M., Goldman, R.D., Louvard, D., Vignjevic, D.M., 2010. Actin, microtubules, and vimentin intermediate filaments cooperate for elongation of invadopodia. J. Cell Biol. 189 (3), 541–556. https://doi.org/10.1083/jcb.200909113.

Shin, D., Athanasiou, K., 1999. Cytoindentation for obtaining cell biomechanical properties. J. Orthop. Res. 17 (6), 880–890. https://doi.org/10.1002/jor.1100170613.

Sneddon, I.N., 1951. Fourier Transforms. McGraw-Hill.

Sneddon, I.N., 1965. The relation between load and penetration in the axisymmetric boussinesq problem for a punch of arbitrary profile. Int. J. Eng. Sci. 3 (1), 47–57. https://doi.org/10.1016/0020-7225(65)90019-4.

Suresh, S., 2007. Biomechanics and biophysics of cancer cells. Acta Biomater. 3 (4), 413–438. https://doi.org/10.1016/j.actbio.2007.04.002.

Tseng, Y., Kole, T.P., Wirtz, D., 2002. Micromechanical mapping of live cells by multiple-particle-tracking microrheology. Biophys. J . 83 (6), 3162–3176. https://doi.org/10.1016/S0006-3495(02)75319-8.

Unnikrishnan, G.U., Unnikrishnan, V.U., Reddy, J.N., 2007. Constitutive material modeling of cell: a micromechanics approach. J. Biomech. Eng. 129 (3), 315–323. https://doi.org/10.1115/1.2720908.

Vichare, S., Inamdar, M.M., Sen, S., 2012. Influence of cell spreading and contractility on stiffness measurements using AFM. Soft Matter 8 (40), 10464–10471. https://doi.org/10.1039/C2SM26348C.

Wang, N., Tolić-Nørrelykke, I.M., Chen, J., Mijailovich, S.M., Butler, J.P., Fredberg, J.J., Stamenović, D., 2002. Cell prestress. I. Stiffness and prestress are closely associated in adherent contractile cells. Am. J. Physiol.-Cell Physiol. 282 (3), C606–C616. https://doi.org/10.1152/ajpcell.00269.2001.

Wolf, K., Wu, Y.I., Liu, Y., Geiger, J., Tam, E., Overall, C., Stack, M.S., Friedl, P., 2007. Multi-step pericellular proteolysis controls the transition from individual to collective cancer cell invasion. Nat. Cell Biol. 9 (8), 893–904. https://doi.org/10.1038/ncb1616.

Xu, W., Chahine, N., Sulchek, T., 2011. Extreme hardening of PDMS thin films due to high compressive strain and confined thickness. Langmuir 27 (13), 8470–8477. https://doi.org/10.1021/la201122e.

Xu, W., Mezencev, R., Kim, B., Wang, L., McDonald, J., Sulchek, T., 2012. Cell stiffness is a biomarker of the metastatic potential of ovarian cancer cells. PLoS One 7 (10), e46609.

Yamauchi, K., Yang, M., Jiang, P., Yamamoto, N., Xu, M., Amoh, Y., Tsuji, K., Bouvet, M., Tsuchiya, H., Tomita, K., Moossa, A.R., Hoffman, R.M., 2005. Real-time in vivo dual-color imaging of intracapillary cancer cell and nucleus deformation and migration. Cancer Res. 65 (10), 4246–4252. https://doi.org/10.1158/0008-5472.CAN-05-0069.

Zhang, M., Zheng, Y.P., Mak, A.F., 1997. Estimating the effective Young's modulus of soft tissues from indentation tests—Nonlinear finite element analysis of effects of friction and large deformation. Med. Eng. Phys. 19 (6), 512–517. https://doi.org/10.1016/s1350-4533(97)00017-9.

Zink, D., Fischer, A.H., Nickerson, J.A., 2004. Nuclear structure in cancer cells. Nat. Rev. Cancer 4 (9), 677–687. https://doi.org/10.1038/nrc1430.